

# Multiple Instance Neural Networks Based on Sparse Attention for Cancer Detection using T-cell Receptor Sequences

Younghoon Kim<sup>1</sup>, Tao Wang<sup>2,3</sup>, Danyi Xiong<sup>4</sup>, Xinlei Wang<sup>4</sup>, and Seongoh Park<sup>\*5</sup>

<sup>1</sup>Department of Industrial and Management Systems Engineering, Kyung Hee University, Gyeonggi, Korea

<sup>2</sup>Quantitative Biomedical Research Center, Department of Population and Data Sciences, University of Texas Southwestern Medical Center

<sup>3</sup>Center for the Genetics of Host Defense, University of Texas Southwestern Medical Center

<sup>4</sup>Department of Statistical Science, Southern Methodist University

<sup>5</sup>School of Mathematics, Statistics and Data Science, Sungshin Women's University, Seoul, Korea

August 10, 2022

## Abstract

Early detection of cancers has been much explored due to its paramount importance in biomedical fields. Among different types of data used to answer this biological question, studies based on T cell receptors (TCRs) are under recent spotlight due to the growing appreciation of the roles of the host immunity system in tumor biology. However, the one-to-many correspondence between a patient and multiple TCR sequences hinders researchers from simply adopting classical statistical/machine learning methods. There were recent attempts to model this type of data in the context of multiple instance learning (MIL). Despite the novel application of MIL to cancer detection using TCR sequences and the demonstrated adequate performance in several tumor types, there is still room for improvement, especially for certain cancer types. Furthermore, explainable neural network models are not fully investigated for this application. In this article, we propose multiple instance neural networks based on sparse attention (MINN-SA) to

---

\*To whom all correspondence should be addressed. Email: [spark6@sungshin.ac.kr](mailto:spark6@sungshin.ac.kr)

enhance the performance in cancer detection and explainability. The sparse attention structure drops out uninformative instances in each bag, achieving both interpretability and better predictive performance in combination with the skip connection. Our experiments show that MINN-SA yields the highest area under the ROC curve (AUC) scores on average measured across 10 different types of cancers, compared to existing MIL approaches. Moreover, we observe from the estimated attentions that MINN-SA can identify the TCRs that are specific for tumor antigens in the same T cell repertoire.

**Keywords:** Multiple instance learning; instance selection; primary instance; sparse-max;

## 1 Introduction

Multiple instance learning (MIL) is a supervised learning task that includes a special structure called a bag in each entity. In MIL, a set of instances in the same bag and their explanatory variables are observed. Though they share an observed bag-level response (bag label), instances may not have an individual instance-level response that one observes in traditional single-instance learning. Supervised MIL tasks can be classified by types of the label; multiple instance classification (MIC) if the label takes its value on a discrete space, and multiple instance regression (MIR) if on a set of (non-discrete) real numbers. Most MIL applications are MIC, including remote sensing (Trabelsi and Frigui, 2019; Wang et al., 2008), computer vision (Sun et al., 2016), sentimental analysis (Angelidis and Lapata, 2018), and especially biology (Bandyopadhyay et al., 2015; Gao and Ruan, 2017; Xiong et al., 2021). In the meanwhile, MIR has relatively scarce literature. We refer readers to Carbonneau et al. (2018) for more examples in MIC and Park et al. (2020) in MIR.

Motivated by such applications in MIC, researchers have proposed a collection of methods to answer scientific questions arising from diverse real-life problems. Many of those are established by extending classical machine learning algorithms such as support vector machines (Andrews et al., 2003a; Gärtner et al., 2002; Ray and Craven, 2005; Zhang et al., 2007), K-nearest neighbors (Carbonneau et al., 2018; Wang and Zucker, 2000), and gradient boosting (Babenko et al., 2008). The key concepts underlying their extensions are reviewed by Amores (2013) where the author proposed a new taxonomy based on how a method handles a set of instances. More details about the algorithms can be found in Xiong et al. (2021).

In contrast to the diversity found in methodology and application, as pointed out in Carbonneau et al. (2018), benchmark MIL datasets have been still limited to predicting binding sites of molecules, image/text classification in literature. For instances, Amores (2013); Car-

bonneau et al. (2018) have conducted a comparative study using typical real data examples so-called Musk (Dietterich et al., 1997), Text (Andrews et al., 2003b), Speaker (Sander-son and Lovell, 2009), Corel (Chen et al., 2006a), Birds (Briggs et al., 2012), Letters (Frey and Slate, 1991), and Tiger/Elephant/Fox (TEF) (Andrews et al., 2003b), which other MIL researches have also used (Asif and ul Amir Afsar Minhas, 2019; Bergeron et al., 2012; Chep-lygina et al., 2015a; Cheung and Kwok, 2006; Ilse et al., 2018; Kim and Torre, 2014; Raykar et al., 2008). In the light of it, there were recent attempts to bring brand-new data under the MIL framework (Ostmeyer et al., 2019; Xiong et al., 2021): T cell receptor sequencing data for cancer detection.

The problem to distinguish normal and cancerous tissues/patients has attracted much attention due to its great significance in biomedical fields for cancer prognosis. To address this biological problem, past works have used medical images (Saba, 2020; Yan et al., 2021), gene expressions (Li et al., 2017; Lu and Han, 2003; Mostavi et al., 2020; Verda et al., 2019), and single nucleotide polymorphisms (SNPs) (Batnyam et al., 2013; Boutorh and Guessoum, 2015; Hajiloo et al., 2013), etc. As the basis for forming predictive models, the recent appreciation of the roles of the host immunity system in tumor biology has motivated researchers to study T cell receptors (TCRs) (Beshnova et al., 2020; Gee et al., 2018; Lu et al., 2021b; Ostmeyer et al., 2019; Xiong et al., 2021). Xiong et al. (2021) predicted the tumor status of patients using TCR sequences. As multiple TCR sequences (instances) are observed together in different T cells in the same patient (tumor or normal), the observations naturally fall into the category of MIL. The authors conducted a benchmarking study to compare MIC algorithms, but they did not treat deep neural networks in depth, thus leaving the performance of neural network models under-explored. Though Wang et al. (2018b)’s models are included in comparison, they are not complex enough to learn successfully the underlying structure of the TCR data, thus showing unsatisfactory performance. Ostmeyer et al. (2019) investigated the multiple instance learning task that distinguishes T-cell repertoires between tumor and healthy tissues, but they assumed the standard MIL assumption which does not consider relative importance of instances. Beshnova et al. (2020) proposed a deep learning model called DeepCat that utilizes tumor-specific or non-cancer TCRs, but DeepCat ignores the bag-structure as well as possibly different contributions of TCRs. Another deep learning model, named DeepLION, is proposed by Xu et al. (2022), but DeepLION cannot completely remove unimportant instances in explaining the bag labels.

Towards bridging this gap, we introduce a novel neural network model, titled MINN-SA (Multiple Instance Neural Network based on Sparse Attentions), for cancer detection

based on TCR sequences. The salient part of the proposal is the sparse attention structure that flexibly drops out uninformative instances, thus rendering model interpretation more achievable. Recent works from [Lu et al. \(2021a\)](#); [Rymarczyk et al. \(2021\)](#); [Tourniaire et al. \(2021\)](#); [Widrich et al. \(2020\)](#) also employed an attention structure in their neural networks. However, their attention scores are dense, meaning none of them is exactly 0, so that irrelevant information for bag classification could be involved in extracted features. Moreover, the sparsity pattern considered in [Lu et al. \(2021a\)](#) is based on a simple heuristic that keeps top- $N$  instances with the largest scores, which lacks of optimality and stability in results. In contrast, equipped with the sparsemax function by [Martins and Astudillo \(2016\)](#), MINN-SA adaptively discovers the pattern of sparsity in attention scores. This flexibility is also beneficial to predictive performance, which can be further enhanced by adding the skip connection by [He et al. \(2016\)](#). With this state-of-the-art architecture, we achieve the highest overall AUC scores both in balanced and imbalanced datasets in the cancer detection problem. Our main contributions are summarized as follows:

- We propose a sparse attention-based neural network that drops out uninformative instance per bag, achieving model interpretability.
- MINN-SA outperforms comparative methods in cancer detection based on TCR sequences, achieving the highest AUC scores both in balanced and imbalanced datasets.

The remainder of this paper is organized as follows. Section 2 gives the details of our method. Section 3 presents the experimental setup and results of TCR dataset. Finally, we end in Section 4 with a summary and discussion.

## 2 Methods

### 2.1 Multiple instance learning for cancer detection using TCR sequences

In MIL, an observational unit is a bag (a sample). In bag  $i$  ( $i = 1, \dots, n$ ), each of multiple instances is characterized by a vector  $x_{ij}$  of  $p$  features in  $\mathbb{R}^p$ ,  $j = 1, \dots, m_i$ , and a single label  $y_i$  is tagged on it. The goal of MIL is to estimate a function  $f$  that predicts a bag-level label from a set of instances. Note that this function takes a set of instances as an input, so it should be adaptive to different number of instances for each bag.

In our application, tissue samples are collected either from normal or cancer patients and a set of TCR sequences are identified in each sample by using next generation sequencing

technologies (Xiong et al. (2021); Zhang et al. (2021)). The main task is to determine whether a tissue is cancerous or not based on its TCR sequences. Here, we treat the tissue type as a bag-level label and the set of TCR sequences as multiple instances, all of which are contained together in a patient, or a bag. Under this context, we focus on a binary MIC task and thus restrict a bag label in  $\{0, 1\}$ ; for example, 0 (a negative bag) is non-cancer and 1 (a positive bag) is cancer. To associate a series of unlabeled instances to a bag label, we adopt the primary instance assumption. In other words, it is assumed that a portion of instances, or primary instances, can explain the label while the remaining instances, or non-primary instances, are irrelevant to it. In our contexts, those selected TCRs represent specialized T cells that the human immune system develops against the tumor cells. More specifically, the TCRs recognize the tumor-associated antigens (Lee et al. (1999); Lewis et al. (2003)) or tumor neoantigens (Gubin et al. (2015); Lu et al. (2020); Stevanović et al. (2017)) presented on the surface of the tumor cells, which are markers of the tumor cells and distinguish them from normal epithelial cells.

We utilize the sparse attention in the multiple instance neural networks to detect such meaningful TCRs. The proposed layer selectively reflects instances’ information to an extracted feature vector for final classification. The sparsity enhances the classifier’s performance and the explainability of classification results. Moreover, the proposed method is computationally efficient. The details of the proposed method are presented in the following subsections.

## 2.2 Numeric embeddings of TCR sequences

We describe the process of numeric embedding of TCR sequences carried out in Xiong et al. (2021). TCR sequence is a text string comprising a series of amino acids, which is actually a text string. According to Atchley et al. (2005), each amino acid can be converted to five Atchley (latent) factors that sufficiently represent the attributes of the amino acid. This conversion of a set of TCR sequences returns a Atchley matrix, which is inserted into the TCR encoding algorithm (Lu et al., 2021b; Zhang et al., 2021). The key part of the algorithm is a stacked auto-encoder that takes Atchley matrices and returns a set of vectors of fixed length (30 dimensions) determined by the number of neurons in the bottleneck layer. The encoded numeric representation facilitates the usage of TCR sequence data. Most MIL algorithms are only compatible with the numeric type of data, especially for those methods calculating a distance between instances (or bags). We refer to Xiong et al. (2021) for more information about the data and processing details. In particular, we do not claim any original

contribution to the data.

## 2.3 Neural networks based on sparse attention

We propose a neural network based on sparse attention to solve multiple instance classification problems. The overall structure of our model is illustrated in Figure 1 (a), and we give details of each component in our neural network below.

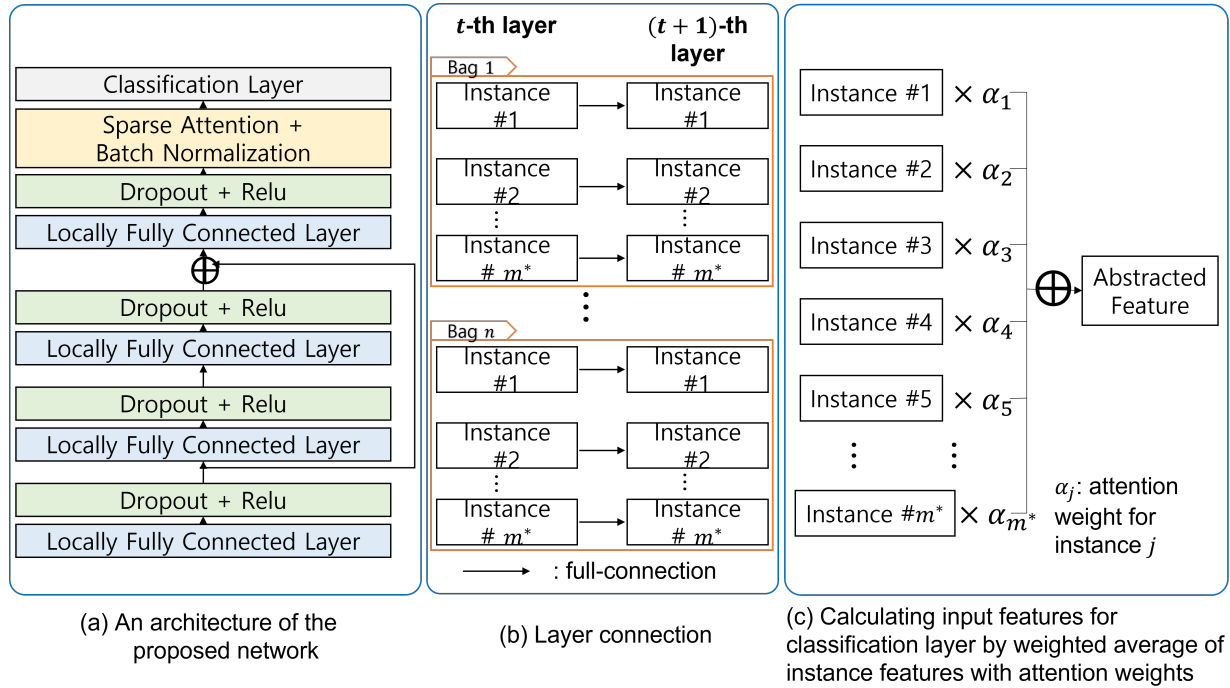


Figure 1: Description of the proposed neural network.

The input size is fixed by  $m^* \times p$  for each of  $n$  bags where  $m^*$  is the hyperparameter that decides the number of instances to be included in modeling. If a bag has fewer instances than  $m^*$ , then an empty part is padded by zeros. Some of bags have larger instance size than  $m^*$ . In the case, we determine the first  $m^*$  instances as our bag instances. Also, we keep using this masking information across the whole process. For ease of handling, one can easily set  $m^*$  by the largest bag size in data. In Section 3, we conduct a sensitivity analysis for choice of the size  $m^*$ .

Each layer consists of  $m^* \times p$  neurons, but they are not fully connected to the activation functions in the previous layer as in the usual fully-connected layer. Instead, we build the full connections between neurons within each instance, but not across different instances (see Figure 1 (b)). The weights for a fully connected layer are shared across the instances

to handle the variable number of instances in each bag. Hence, the two consecutive layers are connected by a  $p \times p$  weight matrix (or  $(p + 1) \times (p + 1)$  if a bias term is included). The network deals with the non-linearity in data with the rectified linear unit (ReLU) (Nair and Hinton, 2010). Note that we used fully connected layers rather than convolution layers because the input features are not locally correlated between adjacent features.

We employed the dropout (Srivastava et al., 2014) and skip connection (He et al., 2016) to enhance the predictive performance. The dropout layer is attached after each locally fully-connected layer appears. It randomly forces the output variables to be zero with probability 0.3 while training the network. It is well known that this layer prevents the complex neural network from overfitting on training data. The residual learning framework eases the training of networks with stacked layers. The skip connections in the framework explicitly let the layers fit a residual mapping instead of hoping stacked layers to directly fit a desired underlying mapping denoted by  $\mathcal{H}(x)$ . We let the stacked nonlinear layers fit another mapping of  $\mathcal{F}(x) := \mathcal{H}(x) - x$ . The bypassing path for a gradient mitigates the vanishing gradient issue in neural networks. The empirical studies show that it is easier to optimize the residual mapping than to optimize the original. Thus, we employ the skip connection to enhance the performance of the locally fully-connected neural network with multi-layers. The effect of residual connection is demonstrated in Section 3.5.

The attention layer combines the attention weights  $\{\alpha_j\}_{j=1}^{m^*}$  returned by the sparsemax function (Martins and Astudillo, 2016) with the feature matrix  $Z \in \mathbb{R}^{m^* \times p}$  obtained from the last network layer, ending up with a weighted feature vector  $\tilde{z} = \sum_{j=1}^{m^*} \alpha_j z_j$  where  $z_j$  is the  $j$ -th row of  $Z$  and  $\tilde{z} \in \mathbb{R}^{1 \times p}$  (see Figure 1 (c)). The commonly used softmax function does not pursue exact zeros in the output, but the sparsemax function permits zeros in it. Let  $\Delta^{K-1} := \{p \in \mathbb{R}^K | 1^T p = 1, p \geq 0\}$  be the  $(K - 1)$ -simplex. The sparsemax is a function mapping vectors in  $\mathbb{R}^K$  to probability distributions in  $\Delta^{K-1}$ :

$$\text{sparsemax}(z) := \underset{p \in \Delta^{K-1}}{\operatorname{argmin}} \|p - z\|^2. \quad (1)$$

In our context, the sparsemax function takes attention scores and encourages some of them to be zero if they do not exceed some thresholding value. As shown in Martins and Astudillo (2016), the threshold is adaptively determined from the scores, not manually by users like hard/soft-thresholding functions.

For each bag, two scores, which correspond to classes of tumor and normal tissues, are converted to probabilities, which is easier to interpret. The transition is done by the sigmoid function. The input of classification layer is batch-normalized feature vector  $\tilde{z}^* \in \mathbb{R}^{1 \times p}$

and the output is a scalar. The aggregated feature vector  $\tilde{z}$  may have different means and variances across components, which could hamper the network from learning data stably. Thus, we apply the batch normalization (Ioffe and Szegedy, 2015) to overcome this difficulty.

We should mention the difference between the proposed attention structure and the others from the previous works. Derived from Lu et al. (2021a); Rymarczyk et al. (2021); Tourniaire et al. (2021); Widrich et al. (2020), the attention scores are strictly larger than zero. Thus, it is challenging to discard unimportant or non-primary instances that have little to do with bag classification. In contrast, MINN-SA allows the attention scores to be sparse or have many zeros, meaning that strictly positive weights are only given to the primary instances responsible to bag classification. This is an attractive instance selection because it transparently shows which instances are chosen in model training and thus facilitates one to interpret classification results only depending on the selected instances. Moreover, our selection is more advanced than the elementary top- $N$  rule (Lu et al. (2021a)) and free from tuning parameters often required in thresholding operators.

## 2.4 Computation

We implement the method with a deep learning framework, PyTorch 1.8.1 (Paszke et al., 2019) with CUDA 11.1 (Garland et al., 2008). The computation system consists of Intel i9-10900 CPU, 32GB RAM, and RTX 3090 GPU. It takes 0.01 seconds for each epoch in the training stage. We stop the training after 100 epochs and determine the best performing model during the training procedure. Therefore, the whole training process approximately takes 1 second in our computation system setting. Referring to the computational time results from Xiong et al. (2021), the proposed method is more efficient than other multiple instances learning methods in computation.

## 3 Results

In this section, we showcase our novel model in distinguishing tumor and normal tissue samples from different types of cancers. Different existing methods are compared against our model in terms of predictive accuracy. Moreover, we provide the instance selection result derived from the estimated attention weights. Lastly, we conduct an ablation study to examine contributions of individual components to our model.

The real datasets we analyze are from The Cancer Genome Atlas (TCGA) database, in whole generated by the TCGA Research Network: <https://www.cancer.gov/tcga>. Normal



and healthy tissues are collected for 10 types of cancers listed in Table 1. As mentioned in Section 2.2, these samples are processed through the next generation sequencing, TCR reconstruction techniques, and TCR encoding algorithms so that the genomic data from the donors are converted in numeric vectors.

### 3.1 Setting

To figure out how they behave in different scenarios, we test the comparative models under two scenarios: (1) the balanced case and (2) the imbalanced case. The former has an equal number of positive (tumor) and negative (normal) bags, while the latter sets about 10% of bags to be positive. The balanced data is commonly used and often preferred in machine learning literature. The other one is to capture characteristics of large population cancer screening where few patients have tumors (Fotouhi et al., 2019; Lin and Chen, 2012; Xiong et al., 2021). To create a dataset for each cancer type, we subsample normal and tumor tissues to keep the aimed proportion of positive (tumor) bags. The sample size of each dataset is tabulated in Table 1.

<b>Cancer</b>	<b>BRCA</b>	<b>DLBC</b>	<b>ESCA</b>	<b>KIRC</b>	<b>LUAD</b>
Balance	404	90	332	404	404
Imbalance	225	225	225	225	225
<b>Cancer</b>	<b>LUSC</b>	<b>OV</b>	<b>SKCM</b>	<b>STAD</b>	<b>THYM</b>
Balance	404	404	404	404	216
Imbalance	225	225	225	225	225

Table 1: The sample size for each cancer type. Half of the samples are tumor tissue samples for the balanced case, while about a tenth of them are for the imbalanced case.

For model training and validation, we conduct 10-fold cross validation (CV) to split training and testing datasets. On the testing dataset, the Area Under the Curve (AUC) of each method is calculated based on the Receiver Operating Characteristic (ROC) curve. We follow the same experimental design in the preceding work (Xiong et al., 2021) for fair comparison.

### 3.2 Benchmarking on cancer detection

To benchmark the proposed model, 18 MIC methods are considered, which are listed in Table 2. We refer to Section 3 of Xiong et al. (2021) for a detailed exposition about these methods.

18 comparative methods		
ADeep (Ilse et al., 2018)	BoW (Amores, 2013)	CCE (Zhou and Zhang, 2007)
CkNN (Wang and Zucker, 2000)	EMD-SVM (Zhang et al., 2007)	EMDD (Zhang and Goldman, 2002)
SI-kNN (Carbonneau et al., 2018)	MI-SVM (Andrews et al., 2003a)	miGraph (Zhou et al., 2009)
MILBoost (Babenko et al., 2008)	MILES (Chen et al., 2006b)	MInD (Cheplygina et al., 2015b)
mi-Net (Wang et al., 2018c)	MI-Net (Wang et al., 2018c)	mi-SVM (Andrews et al., 2003a)
NSK-SVM (Gärtner et al., 2002)	SI-SVM (Ray and Craven, 2005)	MINN-SA

Table 2: Abbreviations of 18 comparative methods including the proposed method “MINN-SA” and their original references.

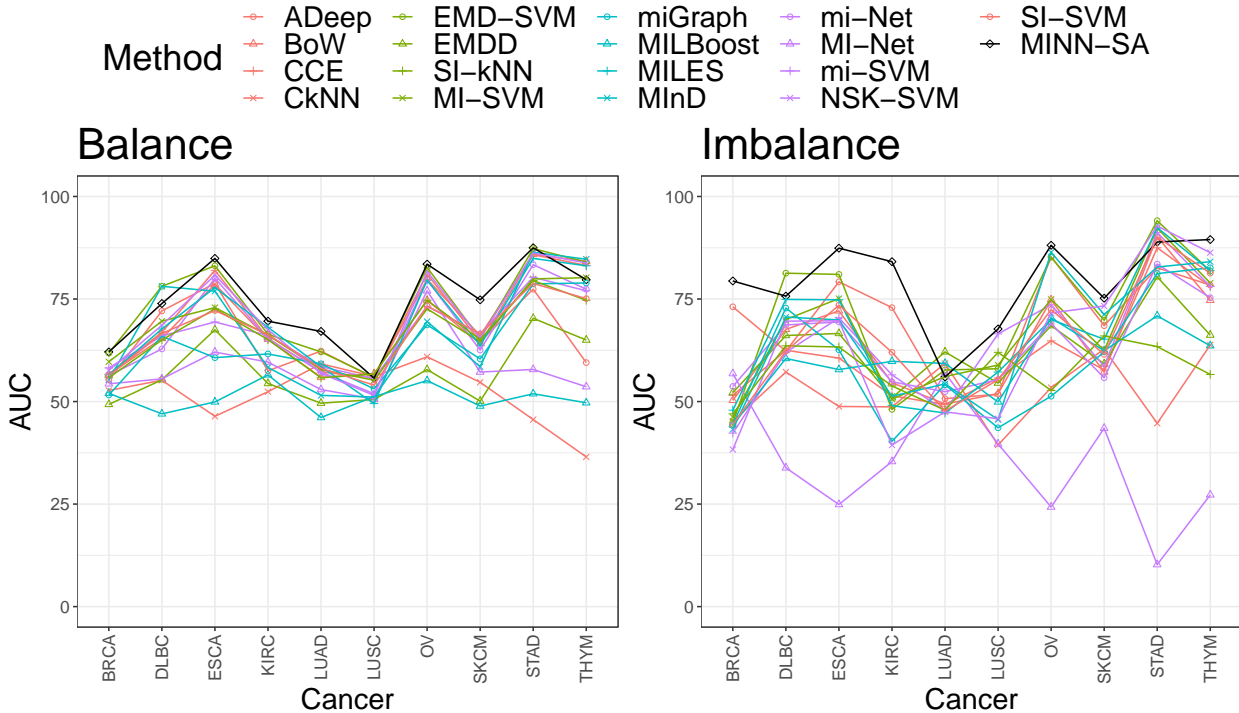


Figure 2: The AUC of all models in comparison across different cancer types. Each point is the average AUC values over 10-fold CV.

Figure 2 shows average AUC values by methods for the ten cancer types. Remarkably, MINN-SA dominates all methods in most of cancer types. Out of 10, MINN-SA wins in 7 types (BRCA, ESCA, KIRC, LUAD, OV, SKCM, STAD) for the balanced case and in different 7 types (BRCA, ESCA, KIRC, LUSC, OV, SKCM, THYM) for the imbalanced case. KIRC, LUAD, SKCM, LUSC are the four most immunogenic cancer types (Wang et al., 2018a), meaning they have a lot of T cell infiltrations. It makes sense these cancer types are among the ones (Wang et al., 2018a) for which our model performs the best,

which investigates TCRs of T cells for classification. Generally, when the class distribution is balanced, each model shows more stable performance (Wang et al., 2018a). The gap between MINN-SA and the second best method is considerably big in BRCA and KIRC datasets for the imbalanced case.

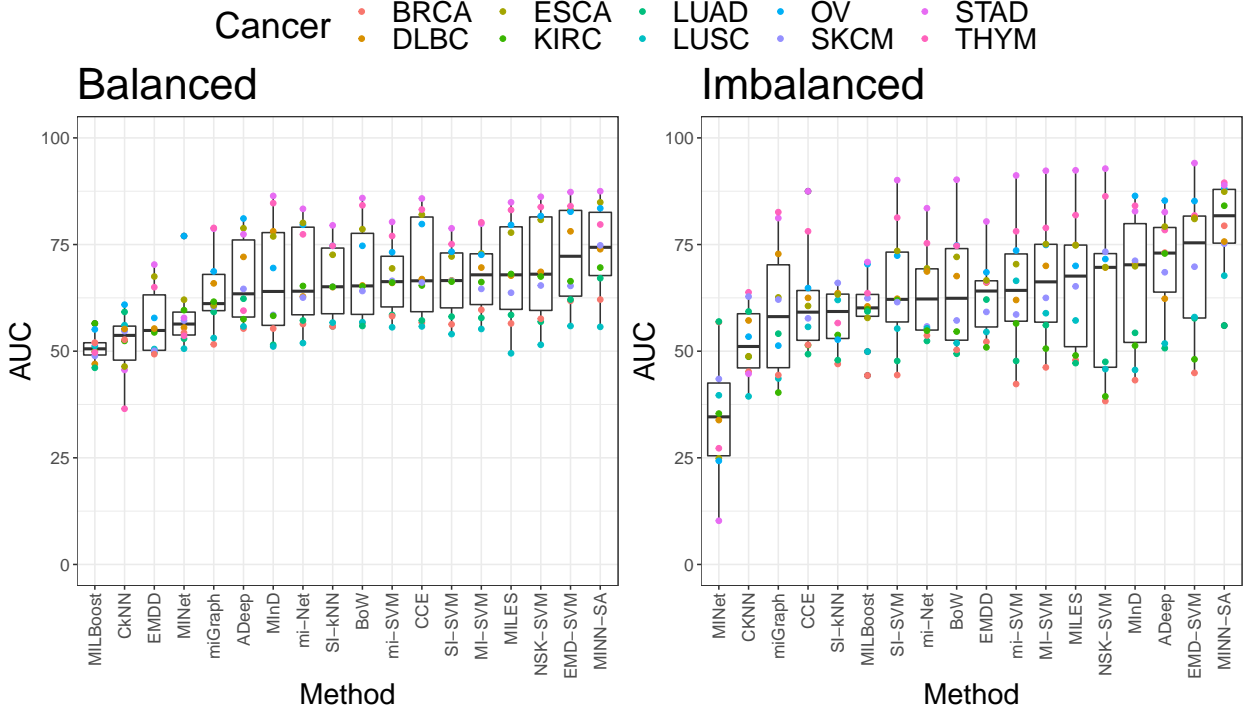


Figure 3: Boxplots of the AUC values across different methods in comparison. They are ordered by median AUC. Each point is the average AUC values over 10-fold CV and different colors are used to show types of cancer.

Figure 3 shows the boxplots of all methods in an ascending order of median AUC. MINN-SA tops in both balanced imbalanced cases, with medians 74.40 and 81.80, respectively, followed by EMD-SVM with 72.20 and 75.40. To demonstrate the superiority of the proposed method over comparative methods, we conducted Wilcoxon signed-rank test on the best and second-best methods with rank statistics. Our proposed method achieves the best performance in terms of average rank over cancers. The average ranks of the proposed method are 2.3 and 2.2 in balanced and imbalanced cases, respectively. The second best method is EMD-SVM, whose average ranks are 2.7 and 5.2. In the balanced case, the p-value is 0.0372, and the p-value for the imbalanced case is 0.0043. Our proposed method outperforms other approaches in both cases with statistical significance.

Moreover, the proposed MINN-SA enjoys interpretable results from selected instances,

which EMD-SVM does not afford. Also, MINN-SA is not very sensitive to class imbalance. Contrary to it, most MIL methods have degraded performance for the imbalanced case, calling for further modifications; for example, data generation or modifying the loss function of the classification model (Huang et al., 2016; Sundin et al., 2019; Yang and Xu, 2020).

### 3.3 Attention of instances

In Figure 4, attention weights of instances are displayed in heatmap. The heatmap is given in a  $n \times m^*$  matrix form where the weights are colored in blue-white spectrum and the masking area (no instances) in gray. The visual inspection demonstrates that the attention weights estimated by MINN-SA are sparser than those by the softmax-based method. For the case based on the softmax function, all instances have strictly positive weights, which is depicted by smooth patterns in the heatmap. Consequently, the dense weights makes the aggregated feature vector from the attention layer depend on redundant information for classification. On the other hand, MINN-SA forces the attention weights of insignificant instances to be exactly zero, which makes decisions of MINN-SA independent of them. In our data, the selected instances are likely the TCRs that are specific for tumor antigens, such as tumor neoantigens or tumor associated antigens, presented on the surface of the tumor cells.

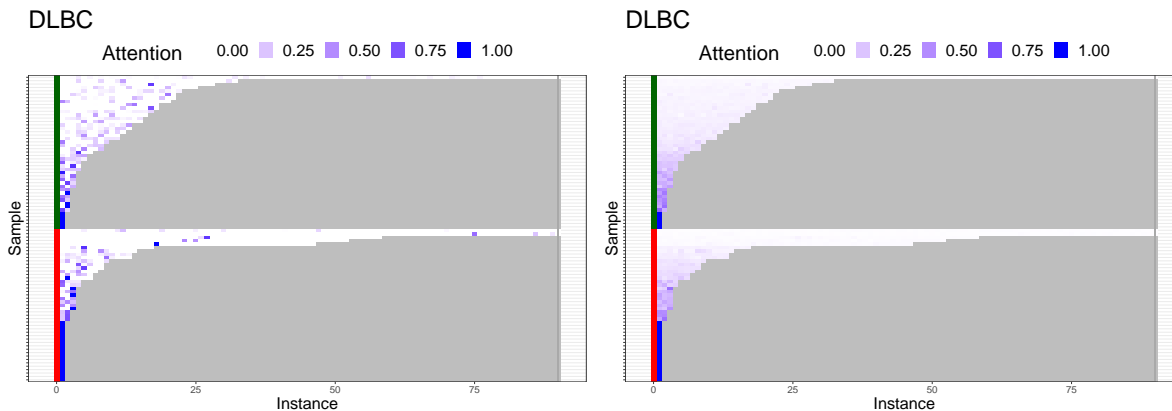


Figure 4: Heatmap of estimated attention weights via the sparsemax (left) and softmax (right) function. Samples are reordered by the number of instances and the masking area (no instances) is colored in gray. Red and green labels indicate tumor and normal samples, respectively. Here, we show the balanced case for DLBC cancer data.

### 3.4 Extracted Features

Figure 5 shows the extracted features before the last classification layer. The heatmap is given in a  $n \times p$  matrix form colored in a blue-yellow spectrum. It can be seen that the

extracted features using the sparsemax function (left) are more activated than using the softmax function (right). Hence, the difference between the features in each observation of the sparsemax case is more distinct than the softmax case. The results demonstrate that the extracted features using the sparsemax function are more informative to characterize the characteristics of each sample. We believe that the sparsity in the proposed attention structure distinguishes the instances responsible for the bag classification so that the aggregated features can accurately discriminate bags in the classification layer.

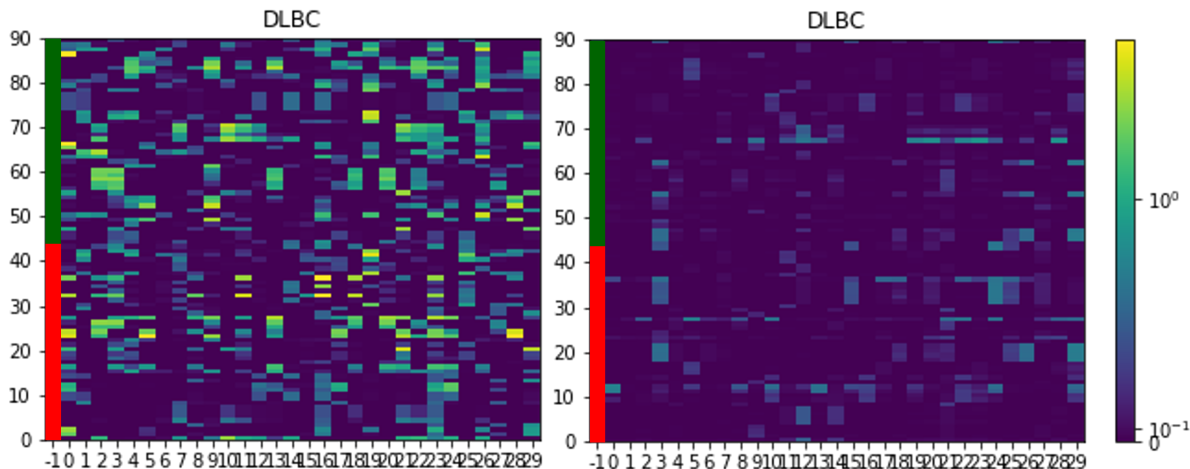


Figure 5: Heatmap of extracted features via the sparsemax (left) and softmax (right) function. Values are min-max normalized and transformed in log-scale. Red and green labels indicate tumor and normal samples, respectively. Here, we show the balanced case for DLBC cancer data.

### 3.5 Ablation study

Firstly, we perform an ablation study to measure contributions of the two components to our neural network: (1) the skip connection and (2) the sparsemax function. Thus, we set a baseline model, denoted by “FC” (short for “fully-connected”), by removing the two components from MINN-SA, and we add each component one after another to “FC”. This leads to the four comparative models shown in Table 3. Note that “FC” is the model used in [Ilse et al. \(2018\)](#), and “Proposed” is MINN-SA.

	<b>FC</b>	<b>Skip</b>	<b>Sparse</b>	<b>Proposed</b>
Skip connection	×	✓	×	✓
Sparsemax layer	×	×	✓	✓
Balance	66.44	69.61	70.33	73.87
Imbalance	70.47	73.79	75.61	79.19

Table 3: Comparison of the four models in the ablation study. Structural difference is checked in the second and third rows where “X” means absence of such structure and “✓” means presence of it. Their average AUC values are summarized in the last two rows.

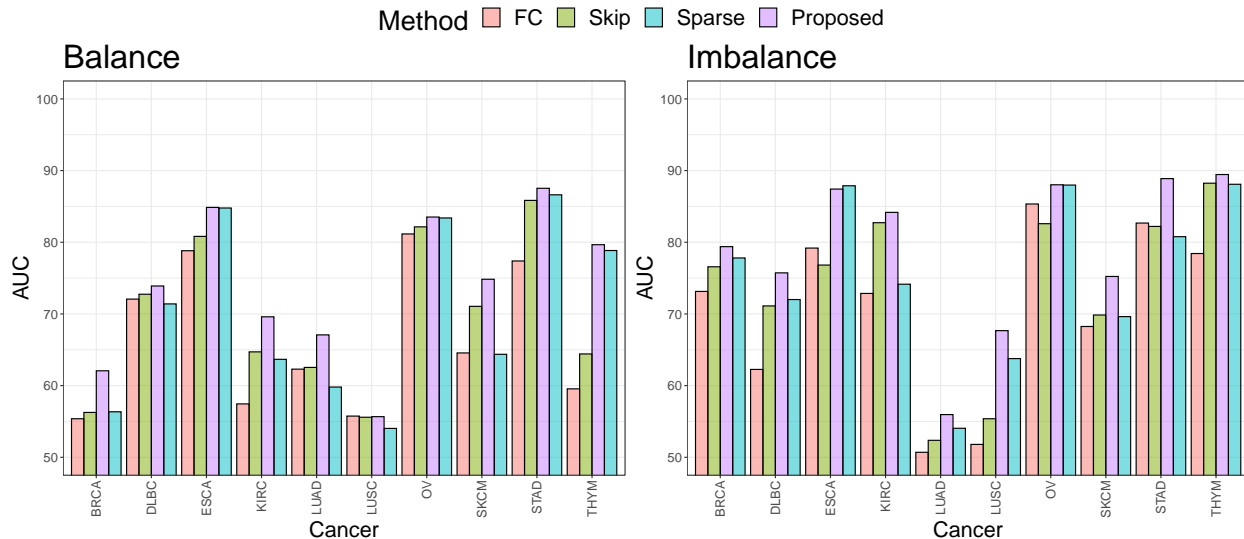


Figure 6: The AUC of four models across different cancer types. Each bar denotes the average AUC values over 10-fold CV.

Figure 6 shows AUC values of the four models for different cancer types. “Proposed” outperforms the others in most cases; otherwise it makes a close second. The superiority of “Proposed” is less distinct in the imbalanced case, but it always takes the first or second place, and thus achieves the highest AUC value 79.19 in average followed by 75.61 (see Table 3). These results lend strong support to the proposed method against the existing multiple instance neural network model by Ilse et al. (2018), a fully-connected neural network based on the softmax function without the skip connection. According to the known phenomenon of immunodominance in the field of immunology (Akram and Inman, 2012; Yewdell and Bennink, 1999), not all instances own necessary information and thus such instances would be better removed for classification by the sparse attention structure. The skip connection also proves valuable for this specific application. Interestingly, the performance is the best

when both skip connection and sparsemax function are utilized together. This phenomenon aligns with the previous study (He et al., 2019) that shows combining regularization tricks can achieve the best classification performance.

In the following ablation study, we assess the sensitivity to the maximum number of instances per bag. We have tried different maximum numbers by  $m^* = 30, 60, \dots, 150$  and their AUC values are reported in Figure 7.

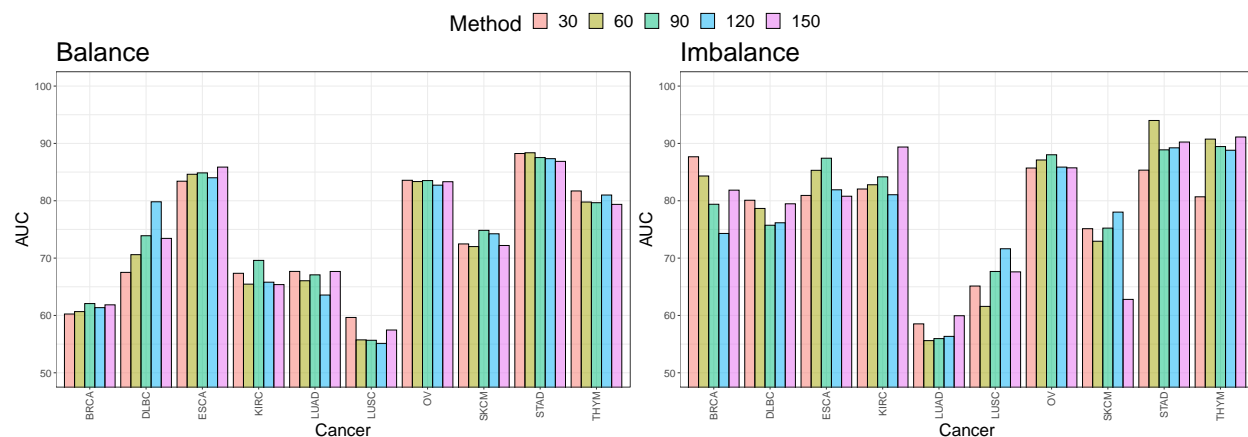


Figure 7: The AUC of the proposed models having different capacity (bag size) of instances across different cancer types. Each bar denotes the average AUC values over 10-fold CV.

The results show that there is no significant difference in classification performance according to the hyperparameter  $m^*$ . This implies that the absolute amount of data increases as  $m^*$  increases, but useful information learned for classification could be limited. However, as shown in Figure 8, bags with more than 30 instances belong to the minority of cases, calling for caution about generalization of this result to other applications. Hence, one should take characteristics of data in hand into account to decide which range of  $m^*$  would be explored. The bag size  $m^*$  is a hyperparameter for the machine learning model and can be optimized by validation procedures such as  $k$ -fold cross-validation.

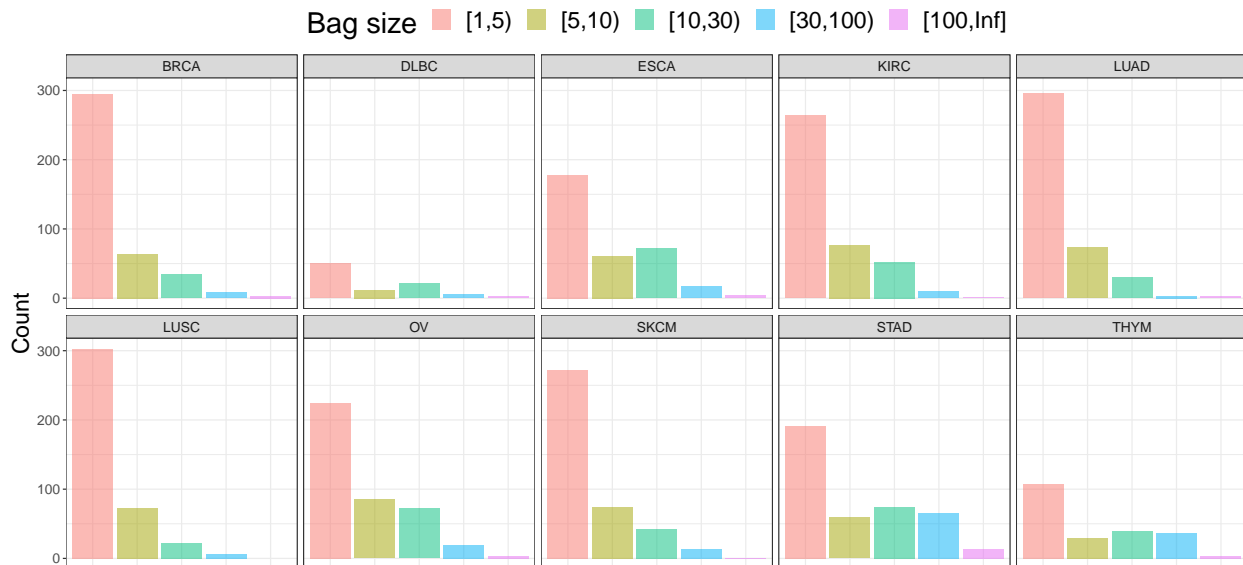


Figure 8: The distribution of bag sizes in the balanced dataset. Most of bags have less than 5 instances, expressing heavy-tailed features.

## 4 Discussion

This paper shows that MINN-SA has improved performance on most cancer types compared to the existing methods in predicting tumor vs. normal tissue samples using TCRs. The results imply that a deep neural network is suitable for multiple instance learning. In contrast, traditional statistical approaches may not work that well, and this is because the deep learning approaches can capture very complicated bag-instance structures. The flexible structures of deep neural networks reflect the bag-instance information efficiently through purely data-driven approaches. For statistical approaches, such bag-instance relationships have to be assumed and sophisticatedly specified. We believe the hand-made specifications are vulnerable to data variations such as cancer types.

Potentially, the proposed model can be also applied to various MIC problems where instances are naturally arranged in sets and having weakly annotated data. MINN-SA produces interpretable results illustrating the importance of instances and thus selecting a subset of primary instances. The applications include biology and chemistry, computer vision, document classification, web mining, reinforcement learning, speech recognition, and time series classification (Carbonneau et al., 2018). Specifically to biology and bioinformatics, the bags consist of complex chemical or biological entities. The interpretable attention results lead to detecting meaningful instances (e.g. compounds, molecules, genes) to characterize biological



properties. Moreover, the binary classification setting could be easily modified for a multi-class classification setting where the final output is calculated by the softmax function and the loss function is defined by a multi-class cross-entropy for optimization.

The instance selection procedure by the sparse attention could be considered a regularization technique commonly used in statistical learning (Hastie et al., 2009). The LASSO (Tibshirani, 1996) is a representative method to select essential features with sparsity. Regression coefficients of LASSO have non-zero or exact zero values by a shrinkage constraint. The features with non-zero coefficients affect the response variations, but the features with zero coefficients have no influence. The sparsity removes redundant feature information in calculating responses. The proposed method and the LASSO share a similar concept of selecting important information from data. The difference is that LASSO selects important features, but the proposed method selects important instances in a bag. The relationship between the sparse and basic attention for MIL is demonstrated by the relationship between LASSO and Ridge regression (Hoerl and Kennard, 1970). Ridge regression is also a shrinkage method, but the coefficients are not forced to be exact zeros. Thus, it is hard to interpret the Ridge regression results regarding feature selection. In the MIL problem, previous methods based on attention are inappropriate for explaining classification results because all the attention values are non-zero.

## Acknowledgement

In loving memory of our late friend Ze Zhang, who was a great company and colleague, we would like to express our deepest gratitude for her kindness and support.

## Funding

Younghoon Kim is supported by NRF-2020R1G1A1101853, Tao Wang and Xinlei Wang are funded by NIH (R01CA258584), Seongoh Park is supported by the Sungshin Women's University Research Grant of H20200131.

## References

Akram, A. and Inman, R. D. (2012). Immunodominance: A pivotal principle in host response to viral infections. *Clinical Immunology*, 143(2):99–115.

- Amores, J. (2013). Multiple instance classification: Review, taxonomy and comparative study. *Artificial Intelligence*, 201:81–105.
- Andrews, S., Tsochantaridis, I., and Hofmann, T. (2003a). Support vector machines for multiple-instance learning. In *Advances in neural information processing systems*, pages 577–584.
- Andrews, S., Tsochantaridis, I., and Hofmann, T. (2003b). Support vector machines for multiple-instance learning. In Becker, S., Thrun, S., and Obermayer, K., editors, *Advances in Neural Information Processing Systems*, volume 15. MIT Press.
- Angelidis, S. and Lapata, M. (2018). Multiple instance learning networks for fine-grained sentiment analysis. *Transactions of the Association for Computational Linguistics*, 6:17–31.
- Asif, A. and ul Amir Afsar Minhas, F. (2019). An embarrassingly simple approach to neural multiple instance classification. *Pattern Recognition Letters*, 128:474–479.
- Atchley, W. R., Zhao, J., Fernandes, A. D., and Drüke, T. (2005). Solving the protein sequence metric problem. *Proceedings of the National Academy of Sciences*, 102(18):6395–6400.
- Babenko, B., Dollár, P., Tu, Z., and Belongie, S. (2008). Simultaneous learning and alignment: Multi-instance and multi-pose learning. In *Workshop on Faces in ‘Real-Life’ Images: Detection, Alignment, and Recognition*.
- Bandyopadhyay, S., Ghosh, D., Mitra, R., and Zhao, Z. (2015). Mbstar: multiple instance learning for predicting specific functional binding sites in microrna targets. *Scientific Reports*, 5(1).
- Batnyam, N., Gantulga, A., and Oh, S. (2013). An efficient classification for single nucleotide polymorphism (snp) dataset. In *Computer and information science*, pages 171–185. Springer.
- Bergeron, C., Moore, G., Zaretzki, J., Breneman, C. M., and Bennett, K. P. (2012). Fast bundle algorithm for multiple-instance learning. *IEEE Transactions on Pattern Analysis and Machine Intelligence*, 34(6):1068–1079.

- Beshnova, D., Ye, J., Onabolu, O., Moon, B., Zheng, W., Fu, Y.-X., Brugarolas, J., Lea, J., and Li, B. (2020). De novo prediction of cancer-associated t cell receptors for noninvasive cancer detection. *Science Translational Medicine*, 12(557):eaaz3738.
- Boutorh, A. and Guessoum, A. (2015). Classification of snps for breast cancer diagnosis using neural-network-based association rules. In *2015 12th International Symposium on Programming and Systems (ISPS)*, pages 1–9.
- Briggs, F., Fern, X. Z., and Raich, R. (2012). Rank-loss support instance machines for mimi instance annotation. In *Proceedings of the 18th ACM SIGKDD International Conference on Knowledge Discovery and Data Mining, KDD '12*, page 534–542, New York, NY, USA. Association for Computing Machinery.
- Carbonneau, M.-A., Cheplygina, V., Granger, E., and Gagnon, G. (2018). Multiple instance learning: A survey of problem characteristics and applications. *Pattern Recognition*, 77:329 – 353.
- Chen, Y., Bi, J., and Wang, J. Z. (2006a). Miles: Multiple-instance learning via embedded instance selection. *IEEE Transactions on Pattern Analysis and Machine Intelligence*, 28(12):1931–1947.
- Chen, Y., Bi, J., and Wang, J. Z. (2006b). Miles: Multiple-instance learning via embedded instance selection. *IEEE Transactions on Pattern Analysis and Machine Intelligence*, 28(12):1931–1947.
- Cheplygina, V., Tax, D. M., and Loog, M. (2015a). Multiple instance learning with bag dissimilarities. *Pattern Recognition*, 48(1):264–275.
- Cheplygina, V., Tax, D. M., and Loog, M. (2015b). Multiple instance learning with bag dissimilarities. *Pattern Recognition*, 48(1):264–275.
- Cheung, P.-M. and Kwok, J. T. (2006). A regularization framework for multiple-instance learning. In *Proceedings of the 23rd International Conference on Machine Learning, ICML '06*, pages 193–200, New York, NY, USA. ACM.
- Dietterich, T. G., Lathrop, R. H., and Lozano-Pérez, T. (1997). Solving the multiple instance problem with axis-parallel rectangles. *Artificial Intelligence*, 89(1):31–71.
- Fotouhi, S., Asadi, S., and Kattan, M. W. (2019). A comprehensive data level analysis for cancer diagnosis on imbalanced data. *Journal of Biomedical Informatics*, 90:103089.

- Frey, P. W. and Slate, D. J. (1991). Letter recognition using holland-style adaptive classifiers. *Machine learning*, 6(2):161–182.
- Gao, Z. and Ruan, J. (2017). Computational modeling of in vivo and in vitro protein-DNA interactions by multiple instance learning. *Bioinformatics*, 33(14):2097–2105.
- Garland, M., Le Grand, S., Nickolls, J., Anderson, J., Hardwick, J., Morton, S., Phillips, E., Zhang, Y., and Volkov, V. (2008). Parallel computing experiences with cuda. *IEEE micro*, 28(4):13–27.
- Gärtner, T., Flach, P. A., Kowalczyk, A., and Smola, A. J. (2002). Multi-instance kernels. In *ICML*, volume 2, page 7.
- Gee, M. H., Han, A., Lofgren, S. M., Beausang, J. F., Mendoza, J. L., Birnbaum, M. E., Bethune, M. T., Fischer, S., Yang, X., Gomez-Eerland, R., Bingham, D. B., Sibener, L. V., Fernandes, R. A., Velasco, A., Baltimore, D., Schumacher, T. N., Khatri, P., Quake, S. R., Davis, M. M., and Garcia, K. C. (2018). Antigen identification for orphan t cell receptors expressed on tumor-infiltrating lymphocytes. *Cell*, 172(3):549–563.e16.
- Gubin, M. M., Artyomov, M. N., Mardis, E. R., and Schreiber, R. D. (2015). Tumor neoantigens: building a framework for personalized cancer immunotherapy. *Journal of Clinical Investigation*, 125(9):3413–3421.
- Hajiloo, M., Damavandi, B., HooshSadat, M., Sangi, F., Mackey, J. R., Cass, C. E., Greiner, R., and Damaraju, S. (2013). Breast cancer prediction using genome wide single nucleotide polymorphism data. *BMC bioinformatics*, 14(13):1–10.
- Hastie, T., Tibshirani, R., Friedman, J. H., and Friedman, J. H. (2009). *The elements of statistical learning: data mining, inference, and prediction*, volume 2. Springer.
- He, K., Zhang, X., Ren, S., and Sun, J. (2016). Deep residual learning for image recognition. In *2016 IEEE Conference on Computer Vision and Pattern Recognition (CVPR)*, pages 770–778.
- He, T., Zhang, Z., Zhang, H., Zhang, Z., Xie, J., and Li, M. (2019). Bag of tricks for image classification with convolutional neural networks. In *Proceedings of the IEEE/CVF Conference on Computer Vision and Pattern Recognition*, pages 558–567.
- Hoerl, A. E. and Kennard, R. W. (1970). Ridge regression: Biased estimation for nonorthogonal problems. *Technometrics*, 12(1):55–67.

- Huang, C., Li, Y., Loy, C. C., and Tang, X. (2016). Learning deep representation for imbalanced classification. In *2016 IEEE Conference on Computer Vision and Pattern Recognition (CVPR)*, pages 5375–5384.
- Ilse, M., Tomczak, J., and Welling, M. (2018). Attention-based deep multiple instance learning. In Dy, J. and Krause, A., editors, *Proceedings of the 35th International Conference on Machine Learning*, volume 80 of *Proceedings of Machine Learning Research*, pages 2127–2136. PMLR.
- Ioffe, S. and Szegedy, C. (2015). Batch normalization: Accelerating deep network training by reducing internal covariate shift. In *International conference on machine learning*, pages 448–456. PMLR.
- Kim, M. and Torre, F. D. L. (2014). Multiple instance learning via gaussian processes. *Data Mining and Knowledge Discovery*, 28(4):1078–1106.
- Lee, P. P., Yee, C., Savage, P. A., Fong, L., Brockstedt, D., Weber, J. S., Johnson, D., Swetter, S., Thompson, J., Greenberg, P. D., et al. (1999). Characterization of circulating t cells specific for tumor-associated antigens in melanoma patients. *Nature medicine*, 5(6):677–685.
- Lewis, J. D., Reilly, B. D., and Bright, R. K. (2003). Tumor-associated antigens: From discovery to immunity. *International Reviews of Immunology*, 22(2):81–112.
- Li, Y., Kang, K., Krahn, J. M., Croutwater, N., Lee, K., Umbach, D. M., and Li, L. (2017). A comprehensive genomic pan-cancer classification using the cancer genome atlas gene expression data. *BMC genomics*, 18(1):1–13.
- Lin, W.-J. and Chen, J. J. (2012). Class-imbalanced classifiers for high-dimensional data. *Briefings in Bioinformatics*, 14(1):13–26.
- Lu, M., Pan, Y., Nie, D., Liu, F., Shi, F., Xia, Y., and Shen, D. (2021a). Smile: Sparse-attention based multiple instance contrastive learning for glioma sub-type classification using pathological images. In *MICCAI Workshop on Computational Pathology*, pages 159–169. PMLR.
- Lu, T., Wang, S., Xu, L., Zhou, Q., Singla, N., Gao, J., Manna, S., Pop, L., Xie, Z., Chen, M., Luke, J. J., Brugarolas, J., Hannan, R., and Wang, T. (2020). Tumor neoantigenic-

- ity assessment with csin score incorporates clonality and immunogenicity to predict immunotherapy outcomes. *Science Immunology*, 5(44):eaaz3199.
- Lu, T., Zhang, Z., Zhu, J., Wang, Y., Jiang, P., Xiao, X., Bernatchez, C., Heymach, J. V., Gibbons, D. L., Wang, J., Xu, L., Reuben, A., and Wang, T. (2021b). Deep learning-based prediction of the t cell receptor–antigen binding specificity. *Nature Machine Intelligence*, 3(10):864–875.
- Lu, Y. and Han, J. (2003). Cancer classification using gene expression data. *Information Systems*, 28(4):243–268. Data Management in Bioinformatics.
- Martins, A. and Astudillo, R. (2016). From softmax to sparsemax: A sparse model of attention and multi-label classification. In Balcan, M. F. and Weinberger, K. Q., editors, *Proceedings of The 33rd International Conference on Machine Learning*, volume 48 of *Proceedings of Machine Learning Research*, pages 1614–1623, New York, New York, USA. PMLR.
- Mostavi, M., Chiu, Y.-C., Huang, Y., and Chen, Y. (2020). Convolutional neural network models for cancer type prediction based on gene expression. *BMC medical genomics*, 13(5):1–13.
- Nair, V. and Hinton, G. E. (2010). Rectified linear units improve restricted boltzmann machines. In *ICML*, pages 807–814.
- Ostmeyer, J., Christley, S., Toby, I. T., and Cowell, L. G. (2019). Biophysicochemical Motifs in T-cell Receptor Sequences Distinguish Repertoires from Tumor-Infiltrating Lymphocyte and Adjacent Healthy Tissue. *Cancer Research*, 79(7):1671–1680.
- Park, S., Wang, X., Lim, J., Xiao, G., Lu, T., and Wang, T. (2020). Bayesian multiple instance regression for modeling immunogenic neoantigens. *Statistical Methods in Medical Research*, 29(10):3032–3047. PMID: 32401701.
- Paszke, A., Gross, S., Massa, F., Lerer, A., Bradbury, J., Chanan, G., Killeen, T., Lin, Z., Gimelshein, N., Antiga, L., et al. (2019). Pytorch: An imperative style, high-performance deep learning library. *Advances in neural information processing systems*, 32:8026–8037.
- Ray, S. and Craven, M. (2005). Supervised versus multiple instance learning: An empirical comparison. In *Proceedings of the 22nd international conference on Machine learning*, pages 697–704. ACM.

- Raykar, V. C., Krishnapuram, B., Bi, J., Dundar, M., and Rao, R. B. (2008). Bayesian multiple instance learning: Automatic feature selection and inductive transfer. In *Proceedings of the 25th International Conference on Machine Learning, ICML '08*, page 808–815, New York, NY, USA. Association for Computing Machinery.
- Rymarczyk, D., Borowa, A., Tabor, J., and Zielinski, B. (2021). Kernel self-attention for weakly-supervised image classification using deep multiple instance learning. In *Proceedings of the IEEE/CVF Winter Conference on Applications of Computer Vision*, pages 1721–1730.
- Saba, T. (2020). Recent advancement in cancer detection using machine learning: Systematic survey of decades, comparisons and challenges. *Journal of Infection and Public Health*, 13(9):1274–1289.
- Sanderson, C. and Lovell, B. C. (2009). Multi-region probabilistic histograms for robust and scalable identity inference. In Tistarelli, M. and Nixon, M. S., editors, *Advances in Biometrics*, pages 199–208, Berlin, Heidelberg. Springer Berlin Heidelberg.
- Srivastava, N., Hinton, G., Krizhevsky, A., Sutskever, I., and Salakhutdinov, R. (2014). Dropout: A simple way to prevent neural networks from overfitting. *Journal of Machine Learning Research*, 15(56):1929–1958.
- Stevanović, S., Pasetto, A., Helman, S. R., Gartner, J. J., Prickett, T. D., Howie, B., Robins, H. S., Robbins, P. F., Klebanoff, C. A., Rosenberg, S. A., and Hinrichs, C. S. (2017). Landscape of immunogenic tumor antigens in successful immunotherapy of virally induced epithelial cancer. *Science*, 356(6334):200–205.
- Sun, M., Han, T. X., Liu, M.-C., and Khodayari-Rostamabad, A. (2016). Multiple instance learning convolutional neural networks for object recognition. In *2016 23rd International Conference on Pattern Recognition (ICPR)*, pages 3270–3275.
- Sundin, I., Schulam, P., Siivola, E., Vehtari, A., Saria, S., and Kaski, S. (2019). Active learning for decision-making from imbalanced observational data. In Chaudhuri, K. and Salakhutdinov, R., editors, *Proceedings of the 36th International Conference on Machine Learning*, volume 97 of *Proceedings of Machine Learning Research*, pages 6046–6055. PMLR.
- Tibshirani, R. (1996). Regression shrinkage and selection via the lasso. *Journal of the Royal Statistical Society: Series B (Methodological)*, 58(1):267–288.

- Tourniaire, P., Ilie, M., Hofman, P., Ayache, N., and Delingette, H. (2021). Attention-based multiple instance learning with mixed supervision on the camelyon16 dataset. In *MICCAI Workshop on Computational Pathology*, pages 216–226. PMLR.
- Trabelsi, M. and Frigui, H. (2019). Robust fuzzy clustering for multiple instance regression. *Pattern Recognition*, 90:424–435.
- Verda, D., Parodi, S., Ferrari, E., and Muselli, M. (2019). Analyzing gene expression data for pediatric and adult cancer diagnosis using logic learning machine and standard supervised methods. *BMC bioinformatics*, 20(9):1–13.
- Wang, J. and Zucker, J.-D. (2000). Solving multiple-instance problem: A lazy learning approach.
- Wang, T., Lu, R., Kapur, P., Jaiswal, B. S., Hannan, R., Zhang, Z., Pedrosa, I., Luke, J. J., Zhang, H., Goldstein, L. D., Yousuf, Q., Gu, Y.-F., McKenzie, T., Joyce, A., Kim, M. S., Wang, X., Luo, D., Onabolu, O., Stevens, C., Xie, Z., Chen, M., Filatenkov, A., Torrealba, J., Luo, X., Guo, W., He, J., Stawiski, E., Modrusan, Z., Durinck, S., Seshagiri, S., and Brugarolas, J. (2018a). An empirical approach leveraging tumorgrafts to dissect the tumor microenvironment in renal cell carcinoma identifies missing link to prognostic inflammatory factors. *Cancer Discovery*, 8(9):1142–1155.
- Wang, X., Yan, Y., Tang, P., Bai, X., and Liu, W. (2018b). Revisiting multiple instance neural networks. *Pattern Recognition*, 74:15–24.
- Wang, X., Yan, Y., Tang, P., Bai, X., and Liu, W. (2018c). Revisiting multiple instance neural networks. *Pattern Recognition*, 74:15–24.
- Wang, Z., Radosavljevic, V., Han, B., Obradovic, Z., and Vucetic, S. (2008). *Aerosol Optical Depth Prediction from Satellite Observations by Multiple Instance Regression*, pages 165–176.
- Widrich, M., Schäfl, B., Pavlović, M., Ramsauer, H., Gruber, L., Holzleitner, M., Brandstetter, J., Sandve, G. K., Greiff, V., Hochreiter, S., et al. (2020). Modern hopfield networks and attention for immune repertoire classification. *Advances in Neural Information Processing Systems*, 33:18832–18845.



- Xiong, D., Zhang, Z., Wang, T., and Wang, X. (2021). A comparative study of multiple instance learning methods for cancer detection using t-cell receptor sequences. *Computational and Structural Biotechnology Journal*, 19:3255–3268.
- Xu, Y., Qian, X., Zhang, X., Lai, X., Liu, Y., and Wang, J. (2022). Deeplion: Deep multi-instance learning improves the prediction of cancer-associated t cell receptors for accurate cancer detection. *Frontiers in Genetics*, 13.
- Yan, R., Zhang, F., Rao, X., Lv, Z., Li, J., Zhang, L., Liang, S., Li, Y., Ren, F., Zheng, C., et al. (2021). Richer fusion network for breast cancer classification based on multimodal data. *BMC Medical Informatics and Decision Making*, 21(1):1–15.
- Yang, Y. and Xu, Z. (2020). Rethinking the value of labels for improving class-imbalanced learning. In *Conference on Neural Information Processing Systems (NeurIPS)*.
- Yewdell, J. W. and Bennink, J. R. (1999). Immunodominance in major histocompatibility complex class i-restricted t lymphocyte responses. *Annual Review of Immunology*, 17(1):51–88. PMID: 10358753.
- Zhang, J., Marszałek, M., Lazebnik, S., and Schmid, C. (2007). Local features and kernels for classification of texture and object categories: A comprehensive study. *International journal of computer vision*, 73(2):213–238.
- Zhang, Q. and Goldman, S. A. (2002). Em-dd: An improved multiple-instance learning technique. In *Advances in neural information processing systems*, pages 1073–1080.
- Zhang, Z., Xiong, D., Wang, X., Liu, H., and Wang, T. (2021). Mapping the functional landscape of t cell receptor repertoires by single-t cell transcriptomics. *Nature Methods*, 18(1):92–99.
- Zhou, Z.-H., Sun, Y.-Y., and Li, Y.-F. (2009). Multi-instance learning by treating instances as non-iid samples. In *Proceedings of the 26th annual international conference on machine learning*, pages 1249–1256. ACM.
- Zhou, Z.-H. and Zhang, M.-L. (2007). Solving multi-instance problems with classifier ensemble based on constructive clustering. *Knowledge and Information Systems*, 11(2):155–170.